A Finite Element a-h-Formulation for the Reduced Order Hysteretic Magnetization Model for Composite Superconductors

Julien Dular, Arjan Verweij, and Mariusz Wozniak

***Abstract*—The simulation of transient effects in large-scale superconducting systems with the finite element method is computationally expensive. A Reduced Order Hysteretic Magnetization (ROHM) model has been recently proposed for the computation of the magnetization and loss of composite superconductors. It accounts for the interplay between hysteresis, eddy, and coupling effects, without a need to model the detailed current density distribution, leading to a substantial reduction of simulation time. The ROHM model naturally fits in finite element formulations written in terms of the magnetic field such as the h-ϕ- or ϕ-formulation, but these formulations are not always the optimal choice. For example, in the presence of ferromagnetic materials, one may prefer formulations written in terms of the magnetic flux density. In this context, we introduce in this paper a mixed a-h-formulation that implements the ROHM model. The main advantage of this formulation is the direct use of the constitutive relation defined by the ROHM model, without the need for its inversion. We discuss the computational efficiency of the new formulation compared to a conventional ϕ-formulation, based on a model of a composite superconducting strand.**

***Index Terms*—AC loss, finite element formulations, hysteresis model, magnetization, reduced order method.**

I. Introduction

SUPERCONDUCTING strands and cables under time-varying magnetic field or current generate loss that results from an interplay between hysteresis, eddy, inter-filament coupling, and inter-strand coupling currents. Correctly simulating this loss at the conductor level is important in the design phase of a magnet to assess the cryogenic heat load as well as the temperature and stability margins [1], [2], [3], [4]. The finite element (FE) method is a powerful tool for this purpose. However, simulating these effects in magnet models with a fully detailed conductor description leads to prohibitive simulation times which are completely unrealistic in practice [5], [6], [7].

Homogenization techniques [8] are promising candidates for reducing the computational effort without oversimplifying the problem. They consist in describing the system in terms of the average fields [9] and were mainly developed for non-superconducting applications [10], [11], [12], or for superconducting applications, but without including rate-dependent effects [13], [14], such as coupling currents and eddy currents. The Reduced Order Hysteretic Magnetization (ROHM) model accounts for these rate-dependent effects [15]. Once its parameters are fixed based on reference solutions, this model reproduces the magnetization and loss of composite superconducting strands without requiring the computation of the current density distribution, and hence with a very low computational effort [15].

The ROHM model defines a constitutive relationship between the magnetic field $\boldsymbol{h}$ and the magnetic flux density $\boldsymbol{b} = \boldsymbol{\mathcal{B}}(\boldsymbol{h})$, and therefore fits naturally in FE formulations written in terms of the magnetic field, such as the h-ϕ or the ϕ-formulation, as was introduced in [15]. But in some circumstances, it is preferable to use FE formulations written in terms of the magnetic flux density [16], [17], [18], such as the a-formulation. Such formulations are interesting for models with nonlinear ferromagnetic materials [19], for models featuring rotating parts [17], or to simplify the implementation of source currents [20]. However, implementing the ROHM model in the standard a-formulation would require the inversion of the constitutive relationship $\boldsymbol{b} = \boldsymbol{\mathcal{B}}(\boldsymbol{h})$ [21]. In order to avoid the inversion, we propose in this paper a mixed a-h-formulation, which has the advantages of the a-formulation and is written in terms of the direct constitutive relationship.

In Section II, we briefly recall the basics of the ROHM model. In Section III, we describe its inclusion in two FE formulations: the standard ϕ-formulation and the novel a-h-formulation. Finally, in Section IV, we apply the new formulation on a model representing a composite superconducting strand and discuss its computational performance.

II. ROHM Model

The ROHM model is presented in [15]. It is inspired by the energy-based vector hysteresis model for ferromagnetic materials [22], [23], [24] and consists of a chain of $N \in \mathbb{N}_0$ hysteretic *cells*, as depicted in Fig. 1.

Each cell $k = 1, \dots, N$ defines a relationship between the magnetic field $\boldsymbol{h}$ and a magnetic flux density fraction $\boldsymbol{b}_k$, with weight α_k. The chain of cells defines the total magnetic flux

Received 23 September 2024; revised 11 December 2024, 29 December 2024, and 3 January 2025; accepted 5 January 2025. Date of publication 13 January 2025; date of current version 24 January 2025. *(Corresponding author: Julien Dular.)*

The authors are with CERN, 1211 Geneva, Switzerland (e-mail: julien.dular@cern.ch).

Color versions of one or more figures in this article are available at https://doi.org/10.1109/TASC.2025.3528310.

Digital Object Identifier 10.1109/TASC.2025.3528310

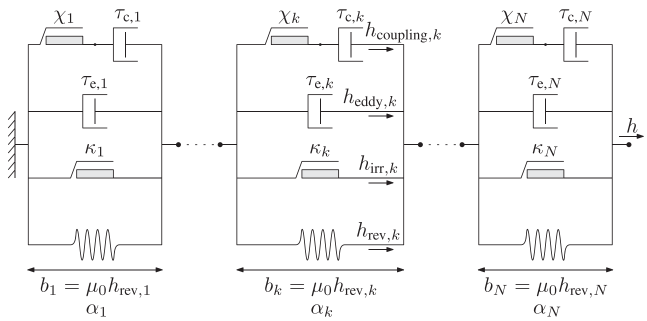

Fig. 1. Mechanical analogy of a chain of hysteretic cells of the ROHM model.

density $\boldsymbol{b}$ with

$$\boldsymbol{b} = \sum_{k=1}^{N} \alpha_k \boldsymbol{b}_k. \tag{1}$$

Each cell is subject to the same magnetic field $\boldsymbol{h}$, but within each cell, $\boldsymbol{h}$ is decomposed into four distinct contributions:

$$\boldsymbol{h} = \boldsymbol{h}_{\mathrm{rev},k} + \boldsymbol{h}_{\mathrm{irr},k} + \boldsymbol{h}_{\mathrm{eddy},k} + \boldsymbol{h}_{\mathrm{coupling},k}. \tag{2}$$

The field $\boldsymbol{h}_{\mathrm{rev},k}$ is associated with stored magnetic energy and is proportional to the magnetic flux density fraction $\boldsymbol{b}_k = \mu_0 \boldsymbol{h}_{\mathrm{rev},k}$, with $\mu_0 = 4\pi \times 10^{-7}$ H/m. It is represented by a linear spring in the mechanical analogy [23] of Fig. 1.

The other three fields, $\boldsymbol{h}_{\mathrm{irr},k}$, $\boldsymbol{h}_{\mathrm{eddy},k}$, and $\boldsymbol{h}_{\mathrm{coupling},k}$, are each associated with different magnetization and loss mechanisms in composite superconductors. The irreversible field $\boldsymbol{h}_{\mathrm{irr},k}$ describes rate-independent hysteresis and obeys

$$\boldsymbol{h}_{\mathrm{irr},k} = \begin{cases} \boldsymbol{h} - \boldsymbol{g}_k, & \text{if } \|\boldsymbol{h} - \boldsymbol{g}_k\| < \kappa_k \\ \kappa_k \, \dot{\boldsymbol{h}}_{\mathrm{rev},k} / \|\dot{\boldsymbol{h}}_{\mathrm{rev},k}\|, & \text{if } \|\boldsymbol{h} - \boldsymbol{g}_k\| = \kappa_k \end{cases} \tag{3}$$

with $\boldsymbol{g}_k = \boldsymbol{h}_{\mathrm{rev},k} + \boldsymbol{h}_{\mathrm{eddy},k} + \boldsymbol{h}_{\mathrm{coupling},k}$ and an irreversibility parameter κ_k (A/m). In the mechanical analogy of Fig. 1, it is represented by a dry-friction element [23].

The eddy field $\boldsymbol{h}_{\mathrm{eddy},k}$ describes eddy currents in normal conducting parts of the superconducting composites and obeys

$$\boldsymbol{h}_{\mathrm{eddy},k} = \tau_{\mathrm{e},k} \dot{\boldsymbol{h}}_{\mathrm{rev},k}, \tag{4}$$

with a relaxation parameter $\tau_{\mathrm{e},k}$ (s). It is represented by a viscous-friction element in Fig. 1 [24].

Finally, the coupling field $\boldsymbol{h}_{\mathrm{coupling},k}$ describes coupling currents and coupled filament magnetization. It obeys

$$\boldsymbol{h}_{\mathrm{coupling},k} = \begin{cases} \tau_{\mathrm{c},k} \dot{\boldsymbol{h}}_{\mathrm{rev},k}, & \text{if } \|\tau_{\mathrm{c},k} \dot{\boldsymbol{h}}_{\mathrm{rev},k}\| < \chi_k \\ \chi_k \, \frac{\dot{\boldsymbol{h}}_{\mathrm{rev},k}}{\|\dot{\boldsymbol{h}}_{\mathrm{rev},k}\|}, & \text{if } \|\tau_{\mathrm{c},k} \dot{\boldsymbol{h}}_{\mathrm{rev},k}\| \geq \chi_k \end{cases} \tag{5}$$

with irreversibility χ_k (A/m) and relaxation $\tau_{\mathrm{c},k}$ (s) parameters. It can be represented by a combination of dry-friction and viscous-friction elements in series, as shown in Fig. 1.

Irreversibility parameters κ_k and χ_k are defined as functions of $\|\boldsymbol{b}\|$ to reproduce the effect of the field-dependent critical current density in superconductors.

The implementation of the ROHM model is described in [15] and is particularly straightforward. The numerical simulation requires to save the two vectors $\boldsymbol{g}_k$ and $\boldsymbol{h}_{\mathrm{rev},k}$ as internal variables. They constitute the memory of the ROHM model.

The values of the model parameters must be determined based on reference simulations of the strand response under field excitations of different amplitudes and rates of change. Once the parameters are fixed, the ROHM model can be used to predict the strand response under arbitrary excitations, within the range of amplitudes and rates of change used to calibrate the parameters.

III. Finite Element Formulations

The ROHM model defines a hysteretic function $\boldsymbol{\mathcal{B}}$ for the constitutive relationship $\boldsymbol{b} = \boldsymbol{\mathcal{B}}(\boldsymbol{h})$, which can be included in a FE framework. We present here two FE formulations suited for the implementation of the ROHM model.

Let us consider a numerical domain Ω. It is decomposed into the domain Ω_{m} containing the superconducting composite, whose magnetic response is to be described by the ROHM model, and the complementary domain, denoted as $\Omega_{\mathrm{m}}^{\mathrm{C}}$. The system can be excited by an external magnetic field via boundary conditions, or by a known source current density field $\boldsymbol{j}_{\mathrm{s}}$ flowing in a domain $\Omega_{\mathrm{s}} \subset \Omega$, modelled as a stranded conducting region [20]. Outside of Ω_{s}, $\boldsymbol{j}_{\mathrm{s}} = \boldsymbol{0}$.

For conciseness, we assume that $\Omega_{\mathrm{m}}^{\mathrm{C}}$ is non-conducting. The extension to conducting cases brings no additional challenge.

In Ω_{m}, magnetization currents (including eddy and coupling currents) are not modelled explicitly but their loss and influence on the surrounding fields are directly described by the ROHM model. The set of equations to solve is therefore:

$$\begin{cases} \operatorname{div} \boldsymbol{b} = 0 \\ \mathbf{curl}\, \boldsymbol{h} = \boldsymbol{j}_{\mathrm{s}} \end{cases} \quad \text{with} \quad \begin{cases} \boldsymbol{b} = \boldsymbol{\mathcal{B}}(\boldsymbol{h}), & \text{in } \Omega_{\mathrm{m}} \\ \boldsymbol{b} = \mu \boldsymbol{h}, & \text{in } \Omega_{\mathrm{m}}^{\mathrm{C}} \end{cases} \tag{6}$$

with μ the magnetic permeability in $\Omega_{\mathrm{m}}^{\mathrm{C}}$, that may be a function of $\boldsymbol{h}$ if $\Omega_{\mathrm{m}}^{\mathrm{C}}$ contains ferromagnetic materials. Time-dependence and induction effects are contained in the ROHM model constitutive law.

Together with appropriate initial and boundary conditions, Eqs. (6) define the strong form of the problem. To be solved numerically with the FE method, a weak form should be defined, and subsequently discretized in space on a FE mesh. The ROHM model equations are time-dependent and the problem must therefore also be discretized in time. Time integration is performed with an implicit Euler scheme.

We propose below two different FE formulations of the strong form of the problem. We use the notation $(\boldsymbol{v}\,,\boldsymbol{w})_{\Omega}$ to represent the integral over Ω of the dot product of any two vector fields $\boldsymbol{v}$ and $\boldsymbol{w}$.

A. ϕ-formulation

The ROHM model fits naturally in formulations written in terms of the magnetic field, such as the h-ϕ-formulation [25]. In a case with no explicit eddy currents, the h-ϕ-formulation can be reduced to a ϕ-formulation [15], [25]. Starting from an initial condition, it consists of finding a magnetic field $\boldsymbol{h} = \boldsymbol{h}_{\mathrm{s}} + \mathbf{grad}\, \phi$ with $\phi \in \Phi(\Omega)$ such that, at subsequent time instants,

$\forall \boldsymbol{h}' = \mathbf{grad}\, \phi'$ with $\phi' \in \Phi_0(\Omega)$,

$$\left(\mu \boldsymbol{h}\,,\boldsymbol{h}'\right)_{\Omega_\mathrm{m}^\mathrm{C}} + \left(\boldsymbol{\mathcal{B}}(\boldsymbol{h})\,,\boldsymbol{h}'\right)_{\Omega_\mathrm{m}} = 0 \tag{7}$$

with $\boldsymbol{h}_\mathrm{s}$ a precomputed source field that satisfies $\mathbf{curl}\, \boldsymbol{h}_\mathrm{s} = \boldsymbol{j}_\mathrm{s}$ in Ω, obtained and defined as described in [20]. The function space $\Phi(\Omega)$ is the subset of $H^1(\Omega)$ satisfying essential boundary conditions, and $\Phi_0(\Omega)$ is the same function space but with homogeneous essential boundary conditions. Elements in $\Phi(\Omega)$ and $\Phi_0(\Omega)$ are discretized with node functions [26].

B. a-h-formulation

The standard a-formulation is written in terms of a magnetic vector potential $\boldsymbol{a}$ related to the magnetic flux density via $\mathbf{curl}\, \boldsymbol{a} = \boldsymbol{b}$. It involves the inverse laws

$$\begin{cases} \boldsymbol{h} = \boldsymbol{\mathcal{B}}^{-1}(\boldsymbol{b}), & \text{in } \Omega_\mathrm{m} \\ \boldsymbol{h} = \nu \boldsymbol{b}, & \text{in } \Omega_\mathrm{m}^\mathrm{C} \end{cases} \tag{8}$$

with $\boldsymbol{\mathcal{B}}^{-1}$ the inverse of the hysteretic function $\boldsymbol{\mathcal{B}}$ and ν the magnetic reluctivity. In a case with no explicit eddy currents, it reads as follows: starting from an initial condition, find $\boldsymbol{a} \in \mathcal{A}(\Omega)$ such that, at subsequent time instants, $\forall \boldsymbol{a}' \in \mathcal{A}_0(\Omega)$,

$$\left(\nu\, \mathbf{curl}\, \boldsymbol{a}\,, \mathbf{curl}\, \boldsymbol{a}'\right)_{\Omega_\mathrm{m}^\mathrm{C}} + \left(\boldsymbol{\mathcal{B}}^{-1}(\mathbf{curl}\, \boldsymbol{a})\,, \mathbf{curl}\, \boldsymbol{a}'\right)_{\Omega_\mathrm{m}} = -\left(\boldsymbol{j}_\mathrm{s}\,,\boldsymbol{a}'\right)_{\Omega_\mathrm{s}} \tag{9}$$

with the known source current density $\boldsymbol{j}_\mathrm{s}$ directly integrated [20] and with $\mathcal{A}(\Omega)$ and $\mathcal{A}_0(\Omega)$ appropriate function spaces discretized with perpendicular edge functions in 2D models [27].

In order to avoid the inversion and to maintain a straightforward implementation of the ROHM model, one can modify the standard a-formulation by introducing in Ω_m an auxiliary field $\boldsymbol{h} \in \mathcal{H}_a(\Omega_\mathrm{m})$ (defined below), and solve the following equations, $\forall \boldsymbol{a}' \in \mathcal{A}_0(\Omega)$ and $\forall \boldsymbol{h}' \in \mathcal{H}_a(\Omega_\mathrm{m})$:

$$\begin{cases} \left(\nu\, \mathbf{curl}\, \boldsymbol{a}\,, \mathbf{curl}\, \boldsymbol{a}'\right)_{\Omega_\mathrm{m}^\mathrm{C}} + \left(\boldsymbol{h}\,, \mathbf{curl}\, \boldsymbol{a}'\right)_{\Omega_\mathrm{m}} = -\left(\boldsymbol{j}_\mathrm{s}\,,\boldsymbol{a}'\right)_{\Omega_\mathrm{s}} \\ \left(\mathbf{curl}\, \boldsymbol{a}\,,\boldsymbol{h}'\right)_{\Omega_\mathrm{m}} - \left(\boldsymbol{\mathcal{B}}(\boldsymbol{h})\,,\boldsymbol{h}'\right)_{\Omega_\mathrm{m}} = 0. \end{cases} \tag{10}$$

This is a mixed formulation with two coupled fields in Ω_m. We call it the a-h-formulation.

Mixed formulations require a careful choice of function spaces in order to avoid instabilities during the numerical simulation [28], [29]. We found that stable results and a robust convergence behavior are obtained with $\mathcal{H}_a(\Omega_\mathrm{m})$ defined as

$$\mathcal{H}_a(\Omega_\mathrm{m}) = \{\boldsymbol{h} = \nu_0\, \mathbf{curl}\, \boldsymbol{u} \;:\; \boldsymbol{u} \in H(\mathbf{curl}; \Omega_\mathrm{m})\} \tag{11}$$

with $\nu_0 = 1/\mu_0$, and $\boldsymbol{u}$ being discretized exactly as the magnetic vector potential $\boldsymbol{a}$, i.e., with perpendicular edge functions, but with a support in Ω_m only. It can be gauged in each connected subdomain of Ω_m by being fixed to zero on an arbitrary point in each subdomain.

C. Implementation Details

The inclusion of the ROHM model in a FE formulation makes the problem nonlinear. An iterative technique is therefore necessary to find an approximate solution at each time step. We use a Newton-Raphson scheme, with a Jacobian matrix $\partial \boldsymbol{\mathcal{B}}/\partial \boldsymbol{h}$ defined as in [15], and a convergence criterion based on the relative change of the total power loss between two successive iterations, as was done in [19], with a relative tolerance equal to $\varepsilon_\mathrm{rel} = 10^{-6}$.

The ROHM model also requires to save the fields $\boldsymbol{g}_k$ and $\boldsymbol{h}_{\mathrm{rev},k}$ at each time step. These fields are discretized with element-wise constant vector functions for both formulations.

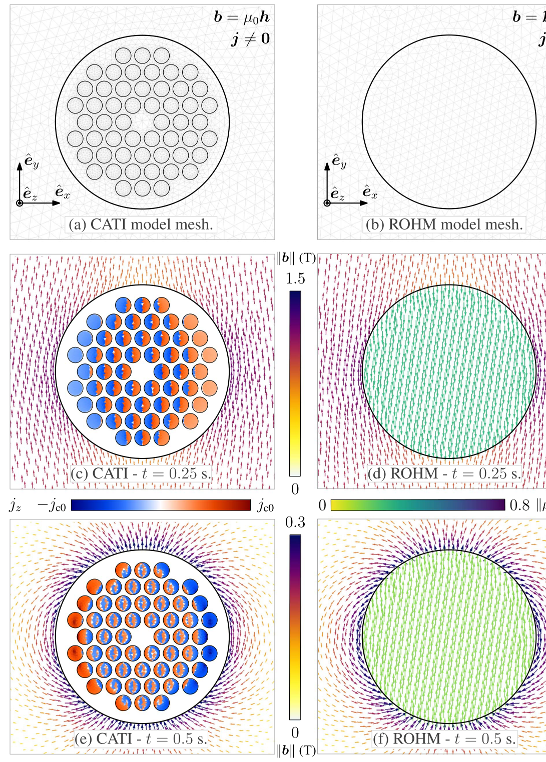

Fig. 2. Application of the ROHM model with the a-h-formulation to reproduce magnetization and loss of a strand without a detailed current density calculation. Frequency: $f = 1$ Hz. (a)-(b) FE meshes. (c)-(d) Solutions at $t = 0.25$ s. (e)-(f) Solutions at $t = 0.5$ s. Arrows outside of the strand represent the magnetic flux density $\boldsymbol{b}$. Colored elements in (c) and (e) represent the z-component of the current density $\boldsymbol{j}$ ($j_{c0} = 3 \times 10^{10}$ A/m^2). Arrows inside the strand in (d) and (f) represent the magnetization $\mu_0 \boldsymbol{m} = \boldsymbol{b} - \mu_0 \boldsymbol{h}$.

IV. Verification and Application

In this section, we present a simple application of the ROHM method in the case of a multifilamentary strand subject to an external field, in order to verify the validity of the a-h-formulation. The FE models are solved by GetDP [30], using Gmsh [31] to generate the geometries and meshes.

We consider a multifilamentary strand of diameter $d = 1$ mm, containing 54 Nb-Ti filaments of diameter 90 µm twisted with a twist pitch length of 19 mm inside a copper matrix. A 2D cross section of the geometry is shown in Fig. 2(a). A magnetic field $h_\mathrm{app}(t) = h_\mathrm{max} \sin(2\pi f t)$ of amplitude $\mu_0 h_\mathrm{max} = 1$ T and frequency f is applied along $\hat{\boldsymbol{e}}_y$. We fix $\boldsymbol{j}_\mathrm{s} = \boldsymbol{0}$ for simplicity.

Reference solutions are obtained with the CATI model [32], implemented in FiQuS [33]. The ROHM model parameters are identified based on reference solutions following the procedure

TABLE I
PARAMETERS OF A CHAIN OF HYSTERETIC CELLS WITH $N = 5$

k (-)	α_k (-)	$\mu_0\bar{\kappa}_k$ (T)	$\tau_{\mathrm{e},k}$ (ms)	$\tau_{\mathrm{c},k}$ (s)	$\mu_0\bar{\chi}_k$ (T)
1	0.23	0.00	0.1	0.00	0.0
2	0.31	0.00	0.1	0.18	1.5
3	0.29	0.25	0.1	0.35	0.7
4	0.13	0.50	0.1	0.35	1.2
5	0.04	0.75	0.1	0.35	1.2

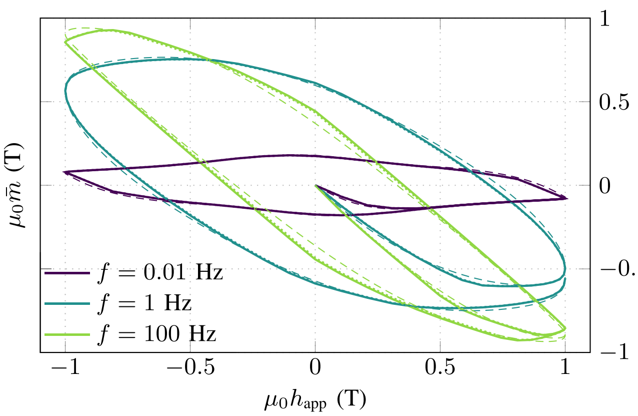

Fig. 3. Average strand magnetization (y-component) for $\mu_0 h_{\max} = 1$ T at different frequencies. Verification of the a-h-formulation (solid curves) compared to the ϕ-formulation (dotted curves) with the ROHM model and $N = 5$. Dashed curves are CATI model solutions, given for reference.

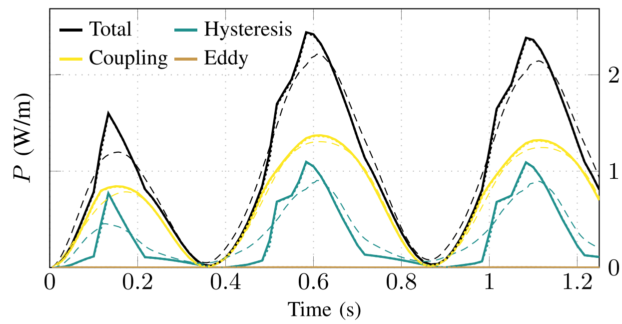

Fig. 4. Instantaneous loss per meter P for $f = 1$ Hz and $\mu_0 h_{\max} = 1$ T and its different contributions (as defined in [15]). Verification of the a-h-formulation (solid curves) compared to the ϕ-formulation (dotted curves) with the ROHM model and $N = 5$. Dashed curves are CATI model solutions, given for reference.

TABLE II
PERFORMANCE FIGURES OF THE ROHM METHOD

Formul.	# DOFs	N	Total # iterations	CPU time (s)
ϕ	2 523	3	240, 231, 217	41, 40, 39
		5	249, 241, 215	53, 53, 48
		8	252, 262, 235	82, 87, 85
a-h	2 945	3	178, 171, 182	29, 27, 30
		5	181, 176, 174	37, 36, 36
		8	180, 182, 177	57, 60, 60

Values for $f = 0.01$, 1, 100 Hz, respectively.

described in [15]. We choose $N = 5$ to describe the strand response, with parameters given in Table I and field-dependent irreversibility parameters $\kappa_k = \bar{\kappa}_k f_\kappa(\|\boldsymbol{b}\|)$ and $\chi_k = \bar{\chi}_k f_\chi(\|\boldsymbol{b}\|)$, with f_κ and f_χ decreasing functions of $\|\boldsymbol{b}\|$, as defined in [15].

Solution fields are represented in Fig. 2 for $f = 1$ Hz at $t = 0.25$ s and $t = 0.5$ s. The magnetization computed by the ROHM model is uniform in this case because of the round shape of the strand. It correctly reproduces the influence of the strand on the surrounding field.

The average magnetization obtained with the ROHM model and both ϕ- and a-h-formulations are compared together, as well as with those obtained with the reference CATI model in Fig. 3 at frequencies f of 0.01 Hz, 1 Hz, and 100 Hz. For the detailed CATI model solution, the average magnetization is computed as in [15]. For the ROHM model solution, the average magnetization is computed as

$$\bar{\boldsymbol{m}} = \frac{1}{a}\int_S \frac{1}{\mu_0}\boldsymbol{\mathcal{B}}(\boldsymbol{h}) - \boldsymbol{h}\,\mathrm{d}S \tag{12}$$

with $a = \pi d^2/4$ the surface area of the cross section S.

The instantaneous loss P and its distinct contributions are shown in Fig. 4 for the $f = 1$ Hz excitation. For the detailed CATI model solution, P is computed by integrating the Joule loss density $p_{\mathrm{J}} = \boldsymbol{j}\cdot(\rho\boldsymbol{j})$ over the strand [15]. For the ROHM model solution, P is obtained by integrating the dissipated magnetic power density p_{m} over the strand, with

$$p_{\mathrm{m}} = \sum_{k=1}^{N} \alpha_k(\boldsymbol{h}_{\mathrm{irr},k} + \boldsymbol{h}_{\mathrm{eddy},k} + \boldsymbol{h}_{\mathrm{coupling},k})\cdot\dot{\boldsymbol{b}}_k. \tag{13}$$

The results of both formulations are almost identical and provide good approximations of the reference magnetization and loss. The cumulative error on the total loss integrated from $t = 0$ to $t = 1.25/f$ is below 3% for both formulations and the three frequencies. The curves of the ROHM model are spiky due to the limited number of cells ($N = 5$) which are triggered one by one when the field varies. Smoother curves can be obtained with a larger number of cells, at the cost of more internal variables to save.

Performance figures of the two formulations with the ROHM method are given in Table II, for 1.25 cycles with 75 time steps. Results for other chains of cells with $N = 3$ and $N = 8$ are also given. The a-h-formulation involves slightly more degrees of freedom (DOFs) but requires on average fewer iterations per time step than the ϕ-formulation to meet the convergence criterion. This results in a lower computational time than for the ϕ-formulation in all tested situations.

Note that in this simple case with uniform magnetization, the mesh for the ROHM method is finer than necessary and could be coarsened. In general, the model can be used on more complex geometries to homogenize a large number of strands, in which case the magnetization is no longer uniform.

V. CONCLUSION

In this article, we presented the a-h- and ϕ-formulations for implementation of the ROHM model. The novel a-h-formulation is more efficient and extends the applicability of the ROHM model to FE models containing nonlinear magnetic materials. This work constitutes a step towards the homogenization of full-scale superconducting systems such as accelerator magnets, in view of a fast and accurate modelling of their transient magneto-thermal response.

Next steps include the investigation of proximity effects due to the magnetization of neighboring conductors in a full-scale magnet model and coupling with transport current effects.

REFERENCES

[1] A. Campbell, "A general treatment of losses in multifilamentary superconductors," *Cryogenics*, vol. 22, no. 1, pp. 3–16, 1982.

[2] M. N. Wilson, *Superconducting Magnets*, U.K.: Clarendon Press, 1983.

[3] E. Ravaioli, T. Mulder, A. Verweij, and M. Wozniak, "Optimizing secondary CLIQ for protecting high-field accelerator magnets," *IEEE Trans. Appl. Supercond.*, vol. 34, no. 5, 2024, Art. no. 4700305.

[4] T. Mulder, B. Bordini, E. Ravaioli, E. Schnaubelt, M. Wozniak, and A. Verweij, "External coil coupled loss induced quench (E-CLIQ) system for the protection of LTS magnets," *IEEE Trans. Appl. Supercond.*, vol. 33, no. 5, Aug. 2023, Art. no. 4702105.

[5] M. Lyly, A. Stenvall, and R. Mikkonen, "Validation of homogenized filament bundle model in AC loss computations," *IEEE Trans. Appl. Supercond.*, vol. 22, no. 3, pp. 4705505–4705505, Jun. 2012.

[6] J. Zhao, Y. Li, and Y. Gao, "3D simulation of AC loss in a twisted multifilamentary superconducting wire," *Cryogenics*, vol. 84, pp. 60–68, 2017.

[7] N. Riva, A. Halbach, M. Lyly, C. Messe, J. Ruuskanen, and V. Lahtinen, "H-phi formulation in sparselizard combined with domain decomposition methods for modeling superconducting tapes, stacks, and twisted wires," *IEEE Trans. Appl. Supercond.*, vol. 33, no. 5, Aug. 2023, Art. no. 4900405.

[8] M. El Feddi, Z. Ren, A. Razek, and A. Bossavit, "Homogenization technique for maxwell equations in periodic structures," *IEEE Trans. Magn.*, vol. 33, no. 2, pp. 1382–1385, Mar. 1997.

[9] A. Marteau et al., "Magnetic field upscaling and B-conforming magnetoquasistatic multiscale formulation," *IEEE Trans. Magn.*, vol. 59, no. 5, 2023, Art. no. 7000404.

[10] G. Meunier, V. Charmoille, C. Guérin, P. Labie, and Y. Maréchal, "Homogenization for periodical electromagnetic structure: Which formulation?," *IEEE Trans. Magn.*, vol. 46, no. 8, pp. 3409–3412, Aug. 2010.

[11] J. Gyselinck, R. Sabariego, and P. Dular, "A nonlinear time-domain homogenization technique for laminated iron cores in three-dimensional finite-element models," *IEEE Trans. Magn.*, vol. 42, no. 4, pp. 763–766, Apr. 2006.

[12] R. V. Sabariego, P. Dular, and J. Gyselinck, "Time-domain homogenization of windings in 3-D finite element models," *IEEE Trans. Magn.*, vol. 44, no. 6, pp. 1302–1305, Jun. 2008.

[13] M. Aleksa, B. Auchmann, S. Russenschuck, and C. Vollinger, "A vector hysteresis model for superconducting filament magnetization in accelerator magnets," *IEEE Trans. Magn.*, vol. 40, no. 2, pp. 864–867, Mar. 2004.

[14] M. Sjöström, B. Dutoit, and J. Duron, "Equivalent circuit model for superconductors," *IEEE Trans. Appl. Supercond.*, vol. 13, no. 2, pp. 1890–1893, Jun. 2003.

[15] J. Dular, A. Verweij, and M. Wozniak, "Reduced order hysteretic magnetization model for composite superconductors," 2024, *arXiv:2409.13653*.

[16] A. Bossavit, "Two dual formulations of the 3-D eddy-currents problem," *COMPEL- Int. J. Computat. Math. Elect. Electron. Eng.*, vol. 4, no. 2, pp. 103–116, 1985.

[17] R. Brambilla, F. Grilli, L. Martini, M. Bocchi, and G. Angeli, "A finite-element method framework for modeling rotating machines with superconducting windings," *IEEE Trans. Appl. Supercond.*, vol. 28, Aug. 2018, Art. no. 5207511.

[18] L. Bortot et al., "A coupled A–H formulation for magneto-thermal transients in high-temperature superconducting magnets," *IEEE Trans. Appl. Supercond.*, vol. 30, no. 5, Aug. 2020, Art. no. 4900911.

[19] J. Dular, C. Geuzaine, and B. Vanderheyden, "Finite-element formulations for systems with high-temperature superconductors," *IEEE Trans. Appl. Supercond.*, vol. 30, no. 3, Apr. 2019, Art. no. 8200113.

[20] P. Dular, P. Kuo-Peng, C. Geuzaine, N. Sadowski, and J. Bastos, "Dual magnetodynamic formulations and their source fields associated with massive and stranded inductors," *IEEE Trans. Magn.*, vol. 36, no. 4, pp. 1293–1299, Jul. 2000.

[21] K. Jacques, R. V. Sabariego, C. Geuzaine, and J. Gyselinck, "Inclusion of a direct and inverse energy-consistent hysteresis model in dual magnetostatic finite-element formulations," *IEEE Trans. Magn.*, vol. 52, no. 3, Mar. 2015, Art. no. 7300304.

[22] A. Bergqvist, "Magnetic vector hysteresis model with dry friction-like pinning," *Physica B: Condens. Matter*, vol. 233, no. 4, pp. 342–347, 1997.

[23] F. Henrotte, A. Nicolet, and K. Hameyer, "An energy-based vector hysteresis model for ferromagnetic materials," *COMPEL-The Int. J. Comput. Math. Elect. Electron. Eng.*, vol. 25, no. 1, pp. 71–80, 2006.

[24] F. Henrotte and K. Hameyer, "A dynamical vector hysteresis model based on an energy approach," *IEEE Trans. Magn.*, vol. 42, no. 4, pp. 899–902, Apr. 2006.

[25] A. Bossavit, *Computational Electromagnetism: Variational Formulations, Complementarity, Edge Elements*. New York, NY, USA: Academic Press, 1998.

[26] A. Bossavit, "Whitney forms: A class of finite elements for three-dimensional computations in electromagnetism," *IEE Proc. A- Phys. Sci., Meas. Instrum., Manage. Educ.- Rev.*, vol. 135, no. 8, pp. 493–500, 1988.

[27] J. Dular, "Standard and mixed finite element formulations for systems with type-II superconductors," PhD Thesis, Univ. Liège, Liège, Belgium, 2023. [Online]. Available: https://orbi.uliege.be/handle/2268/298054

[28] D. Boffi et al. *Mixed Finite Element Methods and Applications*, vol. 44. Berlin, Germany: Springer, 2013.

[29] J. Dular, M. Harutyunyan, L. Bortot, S. Schöps, B. Vanderheyden, and C. Geuzaine, "On the stability of mixed finite-element formulations for high-temperature superconductors," *IEEE Trans. Appl. Supercond.*, vol. 31, no. 6, Sep. 2021, Art. no. 8200412.

[30] P. Dular, C. Geuzaine, F. Henrotte, and W. Legros, "A general environment for the treatment of discrete problems and its application to the finite element method," *IEEE Trans. Magn.*, vol. 34, no. 5, pp. 3395–3398, Sep. 1998.

[31] C. Geuzaine and J.-F. Remacle, "GMSH: A 3D finite element mesh generator with built-in pre-and post-processing facilities," *Int. J. Numer. Methods Eng.*, vol. 79, no. 11, pp. 1309–1331, 2009.

[32] J. Dular, F. Magnus, E. Schnaubelt, A. Verweij, and M. Wozniak, "Coupled axial and transverse currents method for finite element modelling of periodic superconductors," *Supercond. Sci. Technol.*, vol. 37, no. 9, pp. 1–18, 2024.

[33] A. Vitrano, M. Wozniak, E. Schnaubelt, T. Mulder, E. Ravaioli, and A. Verweij, "An open-source finite element quench simulation tool for superconducting magnets," *IEEE Trans. Appl. Supercond.*, vol. 33, no. 5, Aug. 2023, Art. no. 4702006.